DOI: 10.1002/ejic.200801229

Equilibrium and Kinetic Studies of the Reactions between Aqua[1-(2-aminoethyl)piperazine]palladium(II) and Biologically Relevant Nucleophiles

Tanja Soldatović,[a,b] Mohamed Shoukry,[a,c] Ralph Puchta,[a,d] Živadin D. Bugarčić,[e] and Rudi van Eldik*[a]

Keywords: Palladium / Kinetics / Reaction mechanisms / N ligands / Equilibrium / Biomolecules / Glutathione / Antitumor agents

The kinetics and mechanism of the complex-formation reactions of $[Pd(AEP)(H_2O)]^{2+}$, where AEP stands for 1-(2-aminoethyl)piperazine, with biologically relevant ligands were studied as a function of selected nucleophiles and pH. The reactivity of the ligands follows the sequence L-methionine > guanosine-5′-monophosphate > glycine > inosine >> glutathione. The substitution reactions with glutathione showed two reaction steps in which the first step involves coordination through nitrogen and depends on the nucleophile concentration, whereas the second step involves intramolecular isomerization from N- to S-bonded glutathione and does not depend on the nucleophile concentration. The stoichiometry and stability constants of the formed complexes are also reported, and the concentration distribution of the various complex species was evaluated as a function of pH. The results are discussed in terms of the mechanism of antitumor activity of related platinum complexes.

Introduction

In recent years, work from our groups and others has concentrated on the reactions of Pt^{II} and Pd^{II} complexes with sulfur and nitrogen containing biomolecules,[1–11] which could be of fundamental importance in the understanding of the mechanism of anti-tumor activity of related platinum complexes. Coordination compounds of Pt^{II} and Pd^{II} with various tridentate ligands, including diethylenetriamine (dien) and bis(2-pyridylmethyl)amine (bpma) form stable mononuclear complexes even under very acidic conditions.[5,6] These complexes are useful substrates for kinetic and mechanistic studies, and have been used extensively as model compounds for the first step in the binding of platinum anti-tumor complexes to DNA, thiols or thioethers,[9–11] although the complexes themselves are inactive as anti-tumor agents.

The study of the new triamine complex of *N*-aminoethyl piperazine (AEP) was performed because of two important reasons. Firstly, AEP as amine involves O_6-N···H[12] and/or phosphate-N···H intramolecular hydrogen bonding[13,14] with the Pt-DNA adduct, which favors the interaction with DNA, the main target in chemotherapy. Secondly, the piperazine ring may undergo stacking interaction with the sugar group of DNA, which again favors interaction with DNA. The latter effect is similar to that reported for carboplatin, where the stacking interaction between the cyclobutane ring and the sugar group is part of the increased anti-tumor activity.[15]

For mechanistic studies on the action of Pt^{II} anti-tumor drugs, their Pd^{II} analogues are usually good model compounds since they exhibit a 10^4 to 10^5 fold higher reactivity, whereas their structural and equilibrium behavior is rather similar.[1] As part of our interest in the synthesis, structure and reactivity of coordination complexes of Pd^{II} with chelating ligands,[5,16,17] and with the aim of extending our earlier work in this area, we report here a detailed study on the complex-formation equilibrium and kinetics of monofunctional $[Pd\{1\text{-}(2\text{-aminoethyl})piperazine\}(H_2O)]^{2+}$, $[Pd(AEP)(H_2O)]^{2+}$, with sulfur- and nitrogen-donor biologically relevant ligands. The reactions were studied in

$$[Pd(AEP)(H_2O)]^{2+} + L \underset{k_{-1}}{\overset{k_1}{\rightleftharpoons}} [Pd(AEP)L]^{2+} + H_2O \quad (1)$$

L = L-met, GSH, 5'-GMP, Gly, INO

[a] Inorganic Chemistry, Department of Chemistry and Pharmacy, University of Erlangen-Nürnberg,
Egerlandstrasse 1, 91058 Erlangen, Germany
Fax: +49-9131-8527387
E-mail: vaneldik@chemie.uni-erlangen.de
[b] Department of Bio-Chemical and Medicinal Sciences, The State University of Novi Pazar,
Vuka Karadžića bb, 36300 Novi Pazar, Serbia
[c] Department of Chemistry, Faculty of Science, University of Cairo,
Cairo, Egypt
[d] Computer Chemistry Center, University of Erlangen-Nürnberg, Nägelsbachstr. 25, 91052 Erlangen, Germany
[e] Department of Chemistry, Faculty of Science, University of Kragujevac,
Radoja Domanovića 12, 34000 Kragujevac, Serbia
Supporting information for this article is available on the WWW under http://www.eurjic.org or from the author.

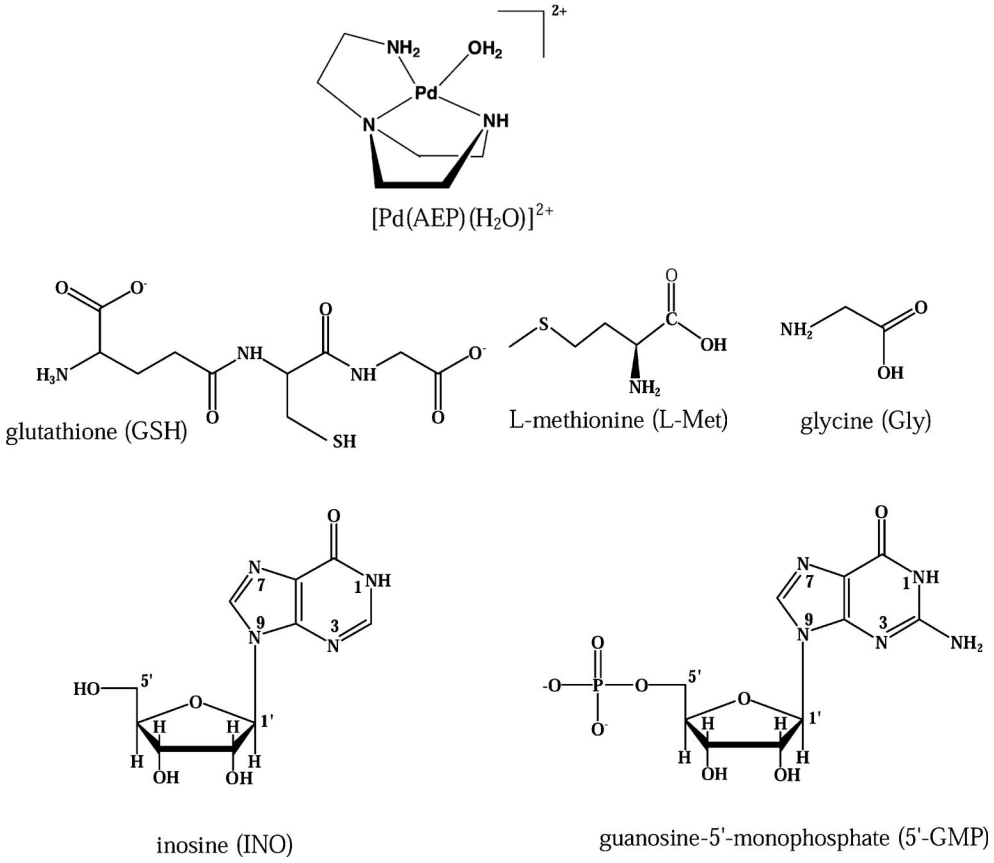

Scheme 1.

0.10 M $NaClO_4$ and 0.01 M acetic acid/acetate buffer at pH 2.5 and 4.75, respectively, as a function of nucleophile concentration at 25 °C according to Equation (1).

The structures of the complex and the selected nucleophiles are shown in Scheme 1.

Results and Discussion

Equilibrium Studies

The acid dissociation constants of the ligands (L) were determined at 25 °C and a constant ionic strength of 0.1 M, which was also used to determine the stability constants of the Pd^{II} complexes. The values obtained are consistent with data reported in the literature.[18]

The $[Pd(AEP)(H_2O)]^{2+}$ complex may undergo hydrolysis in aqueous solution. Its acid-base chemistry was characterized by fitting the potentiometric data to various acid-base models. The best fit was found to be consistent with species of stoichiometric coefficients 10–1 and 20–1. The dimer (20–1) with a single hydroxyl bridge may be formed by the reaction given in Equation (2).

$$[(AEP)Pd(H_2O)]^{2+} + [(AEP)Pd(OH)]^{+} \rightleftarrows [(AEP)Pd\text{-}(\mu\text{-}OH)\text{-}Pd(AEP)]^{3+} + H_2O \quad (2)$$

The equilibrium constant for the dimerization reaction (2) can be calculated by Equation (3) from the formation constants listed in Table 1, and amounts to log K_d = 2.57.

$$\log K_d = \log\beta_{20-1} - \log\beta_{10-1} \quad (3)$$

The pK_a value of coordinated water in $[Pd(diethylenetriamine)H_2O]^{+}$ is 7.74 at 25 °C and 0.5 M ionic strength,[19] compared to 4.68 for coordinated water in $[Pd(AEP)H_2O]^{2+}$. The significantly lower pK_a for $[Pd(AEP)H_2O]^{+}$ results from the chair-to-boat conformational changes in the piperazine ring. This conversion decreases the stability of the $[Pd(AEP)H_2O]^{+}$ complex and consequently increases the electrophilicity of the Pd^{II} center. This in turn strengthens the bond between the Pd^{II} ion and coordinated water and thus lowers the pK_a of coordinated water. This is consistent with earlier data reported for the Ni^{II} complex of 3-[4-(3-aminopropyl)piperazin-1-yl]propylamine.[20]

The species distribution diagram for $[Pd(AEP)(H_2O)]^{2+}$ and its hydrolyzed species is shown in Figure 1. The dimer with a single hydroxyl bridge reaches a maximum concentration of 16% at pH 4.6, whereas the concentration of the mono-hydroxo species (10–1) increases with increasing pH.

Analysis of the titration for the Pd(AEP)-glycine system showed the formation of a 1:1 complex species (see Figure S1, Supporting Information). However, the corresponding data for the L-methionine complex revealed the formation of 1:1 and 2:1 (Pd:ligand) complexes. The formation of the dimeric species (2:1 complex) reflects the high preference of Pd^{II} towards the thioether group of L-methionine. The concentration distribution diagram of the L-methionine complex is given in Figure 2.

Table 1. Formation constants for complexes of $[Pd(AEP)(H_2O)]^{2+}$ with some selected ligands at 25 °C and 0.1 M ionic strength.

Ligand	M	L	H[a]	log β[b]
OH^-	1	0	–1	–4.68 (0.02)
	2	0	–1	–2.11 (0.06)
Glycine	0	1	1	9.76
	1	1	0	10.74 (0.04)
L-Methionine	0	1	1	9.23
	1	1	0	11.86 (0.07)
	2	1	0	16.84 (0.15)
Inosine	0	1	1	8.84
	1	1	0	9.36 (0.02)
	1	1	1	13.17 (0.02)
	2	1	0	14.07 (0.03)
5′-GMP	0	1	1	9.90
	0	1	2	16.22
	1	1	0	10.14 (0.03)
	1	1	2	20.43 (0.03)
	2	1	1	21.23 (0.05)
	2	1	0	16.94 (0.05)
GSH[c]	0	1	1	9.77
	0	1	2	18.60
	0	1	3	22.10
	1	1	0	13.54 (0.06)
	1	1	1	22.01 (0.06)
	1	1	2	25.69 (0.06)
GSH[d]	2	1	0	20.51 (0.08)

[a] M, L and H are the stoichiometric coefficients corresponding to Pd(AEP), ligand and H^+, respectively; the coefficient –1, refers to proton loss. [b] Standard deviations are given in parentheses; sum of square of residuals are less than 5E-7. [c] For 1:1 (Pd:GSH) solution mixture. [d] For 2:1 solution mixture.

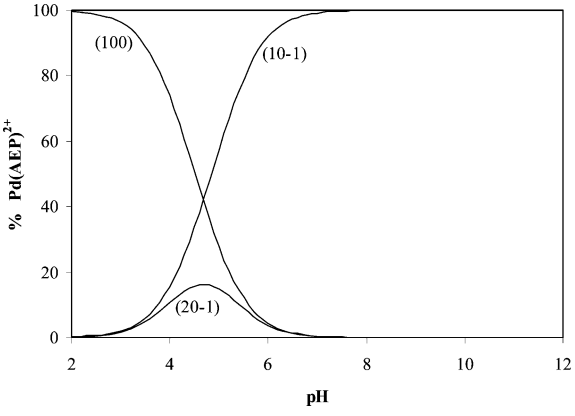

Figure 1. Distribution of various species as a function of pH in the $[Pd(AEP)(H_2O)]^{2+}$ system.

Fitting the potentiometric data for the Pd(AEP)-inosine system indicated the formation of complex species with the stoichiometric coefficients 110, 111 and 210 (see Figure S2, Supporting Information). The protonated species (111) is formed in the acidic pH range and corresponds to the N_7-coordinated complex, where N_1 is protonated. The pK_a value of the protonated species is 3.81, which corresponds

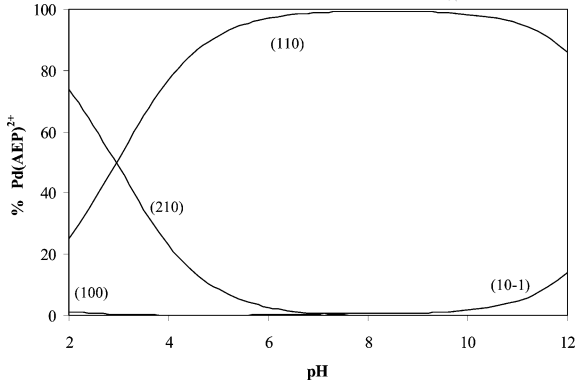

Figure 2. Distribution of various species as a function of pH in the Pd(AEP)-Met system.

to the N_1H group. Acidification of N_1H upon complex-formation is consistent with previous reports.[21] The (210) complex species is formed, most probably, through binding to both the N_7 and N_1 sites. The dimeric species (210) starts to form at pH 2 and reaches the maximum concentration of 58% at pH 3.8. The (110) species starts to form at pH 2 and its concentration increases with increasing pH to reach a maximum degree of formation of 92% at pH 7.6. This indicates that the Pd^{II} ion is coordinated to N_7 in the acidic pH range and then migrates to the N_1 site upon increasing the pH. Also, the (110) species predominates in the physiological pH range.

Analysis of the Pd(AEP)-GMP complex data reveals the formation of the complexes (110), (112), (211) and (210). The complex (112) is formed through coordination to N_7, while the N_1 and phosphate groups are protonated. Also the complexes (210) and (211) are formed through binding of Pd^{II} to both the N_7 and N_1 sites.

The formation of the complex species (210) with 5′-GMP and INO occurs through the equilibrium in Equation (4).

$$\underset{(110)}{Pd(AEP)\text{-}N_7 \sim N_1} + \underset{(100)}{Pd(AEP)} \rightleftharpoons \underset{(210)}{Pd(AEP)\text{-}N_7 \sim N_1\text{-}Pd(AEP)} \quad (4)$$

$$\log K_{eq} = \log\beta_{210} - \log\beta_{110} \quad (5)$$

The equilibrium constant for such a reaction can be calculated using Equation (5) and amounts to log K_{eq} = 6.8 and 4.71 for 5′-GMP and INO, respectively. In the same way, the equilibrium constant for the L-methionine complex was calculated and found to be 4.95.

The equilibrium constant for the 5′-GMP complex is higher than that of the corresponding inosine complex. This may be due to either the involvement of the phosphate group in hydrogen bonding, which will favor complex-formation, or the different coulombic forces involved in the interaction of the tri-negatively charge 5′-GMP ion and the mono-negatively charged inosine ion with $Pd(AEP)^{2+}$. The concentration distribution diagram of the GMP complex is given in Figure 3.

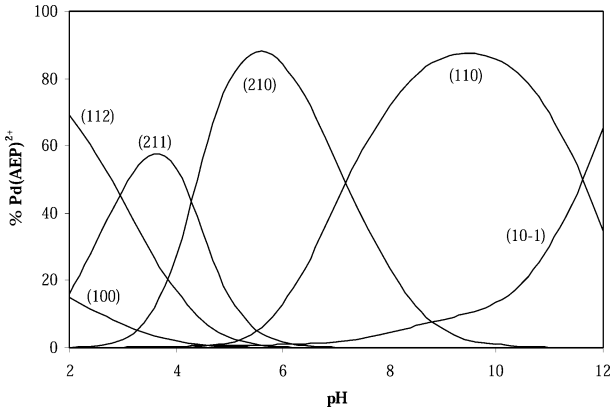

Figure 3. Distribution of various species as a function of pH in the Pd(AEP)-GMP system.

Potentiometric data for a 1:1 mixture of Pd(AEP)-GSH, reveals evidence for the formation of complexes with stoichiometric coefficients (110), (111) and (112). The complex species (110) is most probably formed by binding with the thiolate ion, based on the high affinity of Pd^{II} for S-donor ligands. The concentration distribution diagram, given in Figure 4, shows the formation of the protonated complex (112) with a formation degree of 93% at pH 2. At pH 6, the complex (111) predominates with a concentration of 99%, i.e. the reaction of $Pd(AEP)^{2+}$ goes to completion in the physiological pH range. This may suggest that GSH will compete with DNA for the reaction with the Pd^{II} complex. The potentiometric data for the Pd(AEP)-GSH solution mixture of concentration ratio 2:1, show the formation of the 2:1 complex where both amino and thiolate groups are bound to Pd^{II}; see Figure 4 (b).

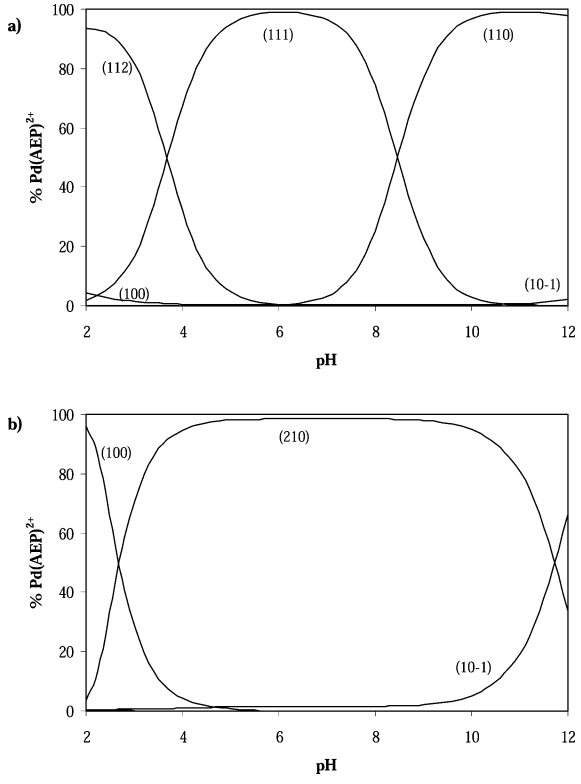

Figure 4. Distribution of various species as a function of pH in the Pd(AEP)-GSH system in the molar ratio 1:1 (**a**) and 2:1(**b**).

Kinetic Studies

The observed pseudo-first-order rate constants, k_{obsd}, depend on the entering nucleophile (Nu) concentration as given in Equation (6).

$$k_{obsd} = k_1[Nu] + k_{-1} \quad (6)$$

A least-squares fit of the data according to Equation (6) resulted in values for the forward anation rate constant, k_1, and reverse aquation rate constant, k_{-1}, according to reaction, Equation (1).[22] Typical experimental results are summarized in Figure 5 and the derived rate constants are summarized in Table 2.

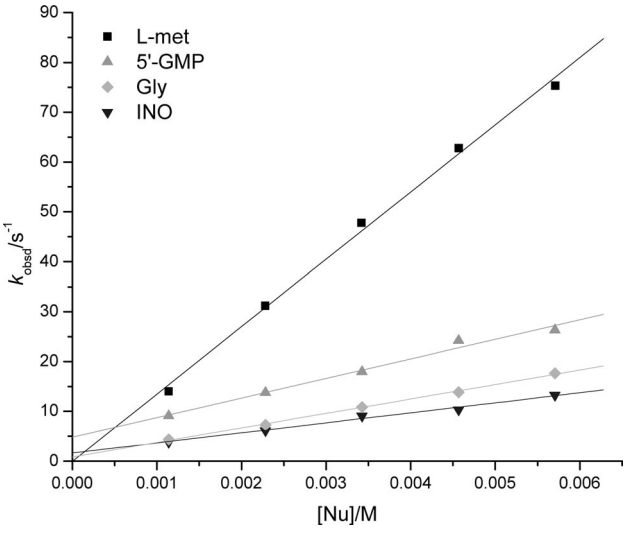

Figure 5. Pseudo-first-order rate constants as a function of nucleophile concentration for the complex-formation reactions of $[Pd(AEP)(H_2O)]^{2+}$ with different nucleophiles at pH 2.5, 25 °C and 0.1 M $NaClO_4$.

Table 2. Rate constants for the reaction of $[Pd(AEP)(H_2O)]^{2+}$ with different nucleophiles at pH = 2.5 (0.10 M $NaClO_4$) and 4.75 (0.01 M acetic acid/acetate buffer).

L	pH	k_1^{298}/M^{-1} s^{-1}	k_{-1}^{298} /s^{-1}	k_2^{298} /s^{-1}
L-Met	2.5	$(13.5 \pm 0.5) \times 10^3$	–	
GSH	2.5	45 ± 2	0.046 ± 0.006	0.030 ± 0.001
GSH	4.75	84 ± 5	0.022 ± 0.002	0.075 ± 0.002
5′-GMP	2.5	$(3.9 \pm 0.3) \times 10^3$	5 ± 1	
5′-GMP	4.75	$(6.4 \pm 0.5) \times 10^3$	0.636 ± 0.002	
Gly	2.5	$(2.9 \pm 0.1) \times 10^3$	0.9 ± 0.3	
INO	2.5	$(2.0 \pm 0.1) \times 10^3$	1.6 ± 0.5	
INO	4.75	$(6.0 \pm 0.3) \times 10^3$	0.133 ± 0.001	

The linear plot of k_{obsd} vs. the concentration of L-methionine passes through the origin (Figure 5), i.e. k_{-1} is negligible and Equation (6) simplifies to $k_{obsd} = k_1[Nu]$. Thus, no significant solvent or reverse reaction path was observed for this particular system, such that direct nucleophilic substitution is the major observed reaction pathway under the selected conditions. In contrast, similar plots for the other studied nucleophiles shown in Figure 5 exhibit significant intercepts, indicating that a back reaction operates in these cases. From the data in Table 2, it can be concluded that L-methionine is the best nucleophile for complex-formation of $[Pd(AEP)(H_2O)]^{2+}$. This can be ascribed to the positive inductive effect of the methyl group on the sulfur donor. Moreover, this result could be very important because Pt–sulfur (thioethers) adducts have been postulated to be a drug reservoir for platinum and may act as intermediate platinum complexes that can be transformed into Pt–DNA adducts.[2,9]

It is well known that thiols are very strong nucleophiles for Pd^{II} complexes.[5] However, in this study we observed an exceptionally low reactivity for glutathione. Spectral changes recorded during the reaction with glutathione (see Figure 6), clearly show an increase in absorbance followed by a subsequent slow decrease in absorbance, typical for two subsequent substitution reactions. The low reactivity, $k_1 = 45 \pm 2\ M^{-1}s^{-1}$, can be explained in terms of coordination of GSH through nitrogen followed by linkage isomerization to coordination through sulfur. If we take into account the pK_a values of GSH, viz. $pK_{a1} = 2.05$, $pK_{a2} = 3.40$, $pK_{a3} = 8.79$ and $pK_{a4} = 9.49$,[23] under our experimental conditions (pH = 2.5 and 4.75), the SH group of GSH will be protonated and prevent direct coordination through sulfur, and so account for the very unusually behavior of this ligand.[5] In addition, the tridentate AEP ligand can to some extent hinder conformational changes that occur during the activation process to form a five-coordinate transition state. Increasing steric hindrance is also expected to slow down the ligand-substitution reactions.

Figure 7 summarizes the experimental data for the two observed reaction steps. Whereas the first step clearly obeys rate law (6) for both pH values, the second reaction step is independent of the entering nucleophile concentration and can be accounted for in terms of an intramolecular isomerization process from N- to S-bonded GSH. The first reaction step (k_1) is somewhat faster at pH 4.75 than at pH 2.5, whereas the intercept (k_{-1}) is larger at pH 2.5 than at pH 4.75. The latter trend can be ascribed to protonation of the N-bonded GSH complex in more acidic solution that will accelerate the reverse aquation reaction. The second reaction step is faster at pH 4.75 than at pH 2.5, viz. $k_2 = 0.075 \pm 0.002\ s^{-1}$ and $0.030 \pm 0.001\ s^{-1}$, respectively, which can be ascribed to a faster isomerization from N- to S-bounded GSH with increasing pH as a result of the deprotonation of the –SH group. The slower rate for the complex-formation reactions with glutathione could be more favorable since the drug resistance of such anti-tumor complexes through the interaction of sulfur-containing proteins will be less efficient both in blood plasma and inside the tumor cells.[2]

Inosine (INO) and guanosine-5′-monophosphate (5′-GMP) can coordinate to metal ions via N_1 and N_7.[31] Under our experimental conditions (pH = 2.5 and 4.75) only the N_7 position of INO ($pK_a = 1.2$) and 5′-GMP will bind to the metal center since the N_1 position is protonated at this pH.[24–27] Binding through the N_7 position in a neutral or weakly acidic medium has been verified.[26] It is also expected that at these pHs the 5′-monophsphate residue of the nucleotide ($pK_a \approx 6$) will not bind to the central metal atom, which could lead to additional complications in the complex-formation mechanism at higher pH.[28] 5′-GMP is more reactive toward the Pd^{II} complex than INO at both studied pH values (see Figures 5 and 8). The intercepts observed for the reactions with 5′-GMP and INO at pH = 4.75 (Table 2) are in both cases smaller due to stronger deprotonation of N_7 and acid-catalyzed aquation is almost suppressed.

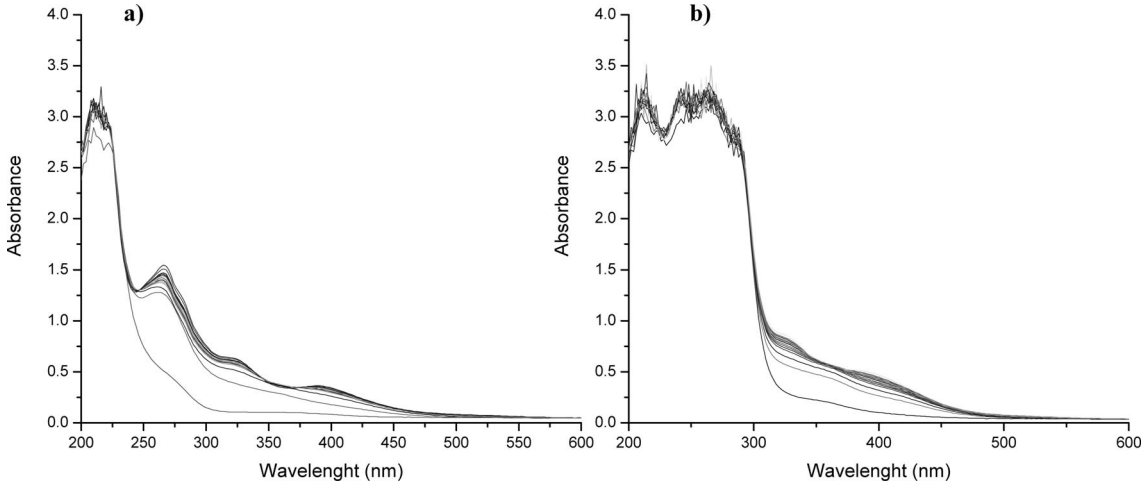

Figure 6. Rapid-scan spectra recorded for the reaction of $[Pd(AEP)(H_2O)]^{2+}$ with glutathione at time intervals of 1 s after mixing at pH 2.5 (**a**) and pH 4.75 (**b**). The increase and subsequent decrease in absorbance indicates the presence of two subsequent reaction steps.

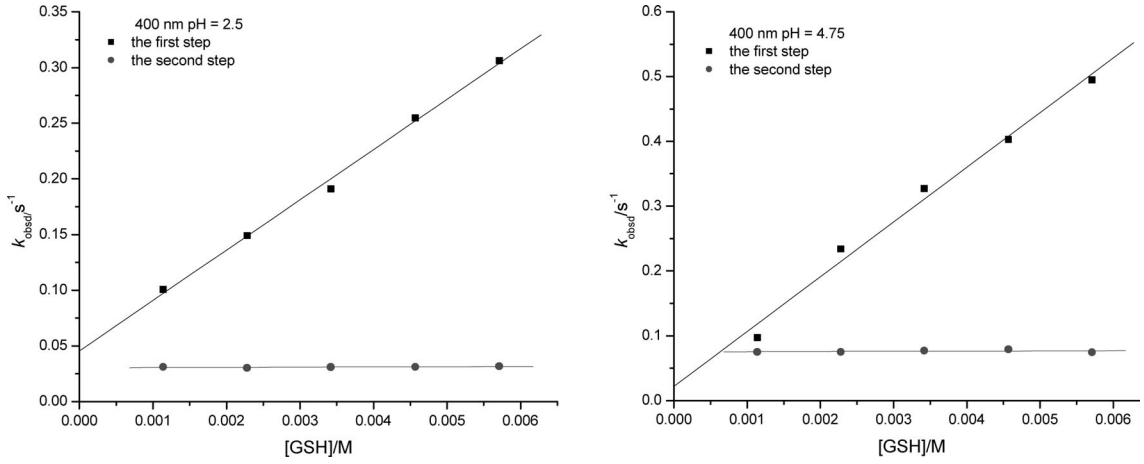

Figure 7. Pseudo-first-order rate constants as a function of nucleophile concentration for the first and second steps of the reaction between $[Pd(AEP)(H_2O)]^{2+}$ and glutathione at different pH and 25 °C.

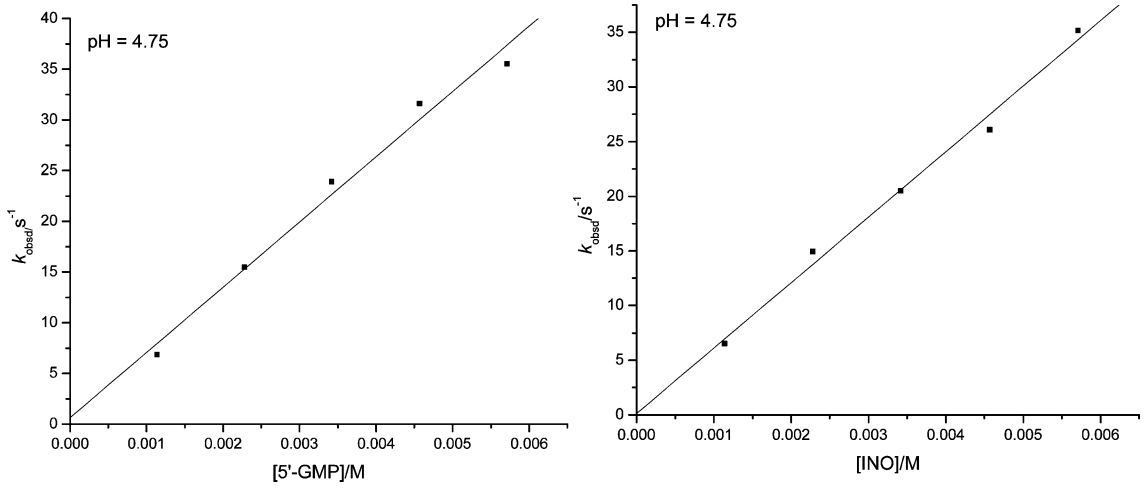

Figure 8. Pseudo-first-order rate constants as a function of nucleophile concentration for complex-formation reactions of $[Pd(AEP)(H_2O)]^{2+}$ at pH 4.75, 25 °C and 0.01 M acetic acid/acetate buffer.

These results clearly indicate that the interaction of Pt^{II} with DNA has important biological implications, since such interactions are thought to be responsible for the anti-tumor activity of platinum drugs.[2,9–11] Also 5′-GMP forms more stable complexes with Pt^{II} than INO.[9] In the case of glycine at pH = 2.5, zwitterions are the reactive species at pH = 2.5 (pK_{a1} = 2.34 and pK_{a2} = 9.60),[23] but still a high reactivity was observed (Table 2). The back reaction (k_{-1} = 0.9 ± 0.3 s^{-1}) is acid-catalyzed because of protonation of the NH_2 group (Figure 5).

The order of reactivity of the biological relevant nucleophiles with the studied Pd^{II} complex is: L-met > 5′-GMP > Gly > INO >> GSH. These results could have implications for the mechanism of action of platinum anti-tumor drugs. Sulfur-donor ligands have a much higher affinity for Pt^{II} complexes than nitrogen-donor ligands and are responsible for the negative effects of platinum anti-tumor activity.[5,6] 5′-GMP can substitute thioeters from Pt-thioether adducts.[10] The low reactivity of GSH is more favorable because it is well known that 5′-GMP cannot substitute thiols from Pt-thiolate adducts and nephrotoxicity has been accounted for in terms of Pt–S (GSH) interactions.[2,9]

Comparison of Thermodynamic and Kinetic Data

A comparison of the stability constants obtained from the potentiometric measurements and those estimated from the kinetic data will now be made. Much of the kinetic work was done in an acidic pH range in order to simplify the speciation of the system. Under this condition, $[Pd(AEP)(H_2O)]^{2+}$ binds to INO and 5′-GMP through the N_7 site, leaving N_1 (INO), and N_1 and phosphate group (5′-GMP) protonated. Under this condition, the stability constants (K_{eq}) for the complexes formed with INO and 5′-GMP were calculated using Equation (7) and (8), respectively.

$$\log K_{eq} = \log\beta_{111} - \log\beta_{011} \quad (7)$$

$$\log K_{eq} = \log\beta_{112} - \log\beta_{012} \quad (8)$$

The log K_{eq} values were found to be 4.33 and 4.21 for INO and 5′-GMP, respectively, and are in reasonable agreement with those estimated from the kinetic data at pH 4.75 (Table 3).

Table 3. Stability constants calculated from kinetic measurements at pH = 2.5 and 4.75 and 25 °C.

L	pH	$K_1(= k_1/k_{-1})$	log K_1	log K_{eq}
GSH	2.5	980 ± 70	2.99	
GSH	4.75	3820 ± 110	3.58	
5′-GMP	2.5	780 ± 125	2.89	
5′-GMP	4.75	10060 ± 50	4.00	4.21
Gly	2.5	3220 ± 800	3.51	
INO	2.5	1250 ± 300	3.10	
INO	4.75	45040 ± 2100	4.65	4.33

It was shown above that N-donor ligands such as DNA constituents have an affinity for $[Pd(AEP)(H_2O)]^{2+}$, which may have important biological implications. However, the preference of Pd^{II} to coordinate to S-donor ligands was demonstrated as shown in Table 2. These results suggest that Pd^{II}–N adducts can easily be converted into Pd–S adducts. Consequently, the equilibrium constant for such conversion is of biological significance.

If we consider inosine as a typical DNA constituent (presented by HL) and glutathione as a typical thiol ligand (presented by H_3B), the equilibria involved in the complex-formation and displacement reactions are:

$$HL \rightleftharpoons H^+ + L^-$$

$$H_3B \rightleftharpoons 3H^+ + B^{3-}$$

$$\underset{(100)}{[Pd(AEP)]^{2+}} + L^- \rightleftharpoons \underset{(110)}{[Pd(AEP)L]^+} \quad (9a)$$

$$\beta_{110}^{[Pd(AEP)L]} = [Pd(AEP)L]/[Pd(AEP)][L] \quad (9b)$$

$$\underset{(100)}{[Pd(AEP)]^{2+}} + B^{3-} \rightleftharpoons \underset{(110)}{[Pd(AEP)B]^-} \quad (10a)$$

$$\beta_{110}^{[Pd(AEP)B]} = [Pd(AEP)B]/[Pd(AEP)][B] \quad (10b)$$

$$[Pd(AEP)(L)]^+ + B^{3-} \overset{K_{eq}}{\rightleftharpoons} [Pd(AEP)(B)^-] + L^- \quad (11)$$

The equilibrium constant for the displacement reaction given in Equation (11) is given by Equation (12).

$$K_{eq} = [Pd(AEP)(B)^-][L^-]/[Pd(AEP)(L)^+][B^{3-}] \quad (12)$$

Substitution from Equations (9b) and (10b) in Equation (12) results in Equation (13).

$$K_{eq} = \beta_{110}^{[Pd(AEP)B]}/\beta_{110}^{[Pd(AEP)L]} \quad (13)$$

logβ_{110} values for the $[Pd(AEP)(L)]^+$ and $[Pd(AEP)B]^-$ complexes taken from Table 1 are 9.36 and 13.54, respectively, and by substitution in Equation (13) results in logK_{eq} = 4.18. In the same way the equilibrium constants for the displacement of coordinated inosine by glycine and L-methionine are found to be log K_{eq} = 1.36 and 2.50, respectively. These values clearly indicate how sulfhydryl ligands such as glutathione are effective in displacing the DNA constituent, i.e., the main target in tumor chemotherapy.

Computer Chemistry

The calculated (B3LYP/LANL2DZp) stabilities of the $[Pd(dien)(H_2O)]^{2+}$ and $[Pd(AEP)(H_2O)]^{2+}$ complex ions are identical within theoretical accuracy, as shown in Figure 9. A comparison of the two structures shows a somewhat elongated Pd–O_{water} bond (0.01 Å), a clear signal for a less electrophilic Pd center. Since in both complexes all coordinating N atoms are formally sp^3 hybridized and only bound to carbon or H atoms, we attribute this reduced electrophilicity to the strain in the eclipsed conformation of the boat shaped piperazine moiety and further to the electron donating effect of the additional CH_2 group of every piperazine

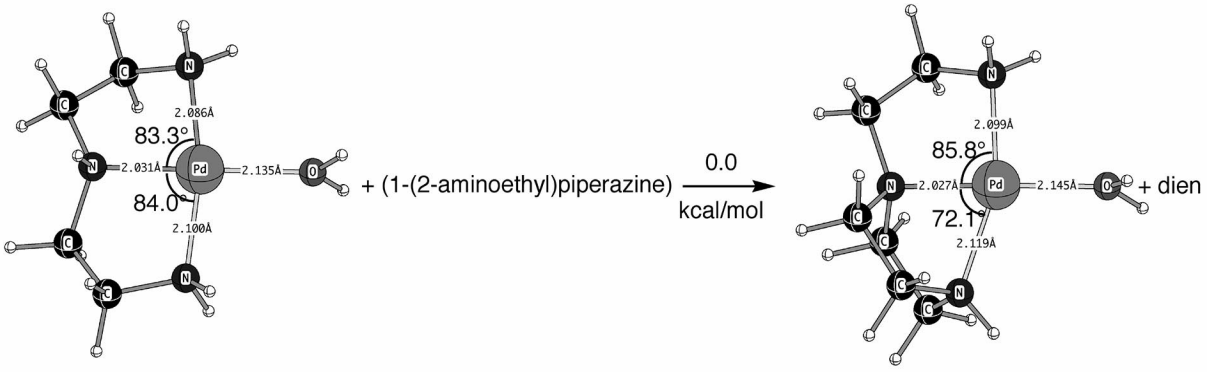

Figure 9. A comparison of the calculated stabilities (B3LYP/LANL2DZp) of the complexes $[Pd(dien)(H_2O)]^{2+}$ and $[Pd(AEP)(H_2O)]^{2+}$.

nitrogen donor. This strain is also seen in the by 12° reduced angle between the two piperazine nitrogen atoms and the Pd^{2+} center. This smaller angle, although causes a somewhat elongated $N_{piperazine}$–Pd bond, as depicted in Figure 9. The reduced electrophilicity can account for the lower reactivity of glutathione towards the $[Pd(AEP)(H_2O)]^{2+}$ complex as compared to $[Pd(dien)(H_2O)]^{2+}$.[5]

Conclusions

The kinetics and mechanism of the complex-formation reactions of $[Pd(AEP)(H_2O)]^{2+}$, where AEP = 1-(2-aminoethyl)piperazine, with biologically relevant ligands were studied as a function of selected nucleophiles and pH. The reactivity of the ligands follows the sequence L-methionine > guanosine-5′-monophosphate > glycine > inosine >> glutathione. This study demonstrated an exceptionally low reactivity for glutathione. Under our experimental conditions (pH = 2.5 and 4.75), the SH group of GSH will be protonated and prevent direct coordination through sulfur. Increasing steric hindrance of the AEP chelate in the complex is also expected to slow down the ligand-substitution reactions for GSH. The first coordination step involves binding of the N-donor, and the second reaction step involves isomerization to S-bonded GSH, which is independent of the entering nucleophile concentration. A comparison of the stability constants obtained from the potentiometric measurements and those estimated from the kinetic data are in good agreement. The calculated (B3LYP/LANL2DZp) Pd–OH_2 bond lengths for $[Pd(dien)(H_2O)]^{2+}$ and $[Pd(AEP)(H_2O)]^{2+}$ suggest the Pd^{II} center in $[Pd(AEP)(H_2O)]^{2+}$ to be less electrophilic than in $[Pd(dien)(H_2O)]^{2+}$, which accounts for the slower substitution reactions observed for $[Pd(AEP)(H_2O)]^{2+}$.

Experimental Section

Chemicals: The nucleophiles inosine (INO), guanosine-5-monophosphate sodium salt hydrate (5′-GMP), L-methionine (L-met), glutathione (GSH) and glycine (Gly), were obtained from Sigma–Aldrich, Acros Organics and Fluka. Nucleophile stock solutions were prepared shortly before use by dissolving the chemicals in purified water. The ligand 1-(2-aminoethyl)piperazine (AEP) was obtained from Fluka and K_2PdCl_4 (97%) was purchased from Strem Chemicals. All other chemicals were of the highest purity commercially available and were used without further purification. Ultra-pure water was used in all experiments in aqueous solution.

Synthesis of [Pd(AEP)Cl]Cl·2H_2O: To an aqueous solution of K_2PdCl_4 (0.82 g, 2.51 mM in 40 mL), 1-(2-aminoethyl)piperazine (0.321 mL, 2.51 mM) was added. The pH was adjusted to between 4 and 5 by the addition of 0.1 M HCl. The intensive yellow solution was stirred overnight at 50 °C, and then evaporated to dryness. Instead of a powder, yellow oil was obtained. The yellow product was precipitated by the addition of methanol (15 mL). Yield: 64.4 mg (1.88 mM, 75%). $C_6H_{19}Cl_2N_3O_2Pd$ (342.54): calcd. C 21.04, H 5.59, N 12.27; found C 21.03, H 4.78, N 11.97. The IR spectrum of [Pd(AEP)Cl]Cl·2H_2O exhibits strong absorption bands at 3438 cm^{-1}, characteristic for water, a strong NH absorption band in the range 3081–3181 cm^{-1}, a δ(NH) band at 1589 cm^{-1}, and a Pd-N absorption at 459 cm^{-1}.

The chloro complex was converted into the corresponding aqua complex in solution by addition of an equivalent of $AgClO_4$, heating to 40–50 °C for 3 h, and removing the precipitated AgCl by filtration through a 0.1 μm pore membrane filter. Care was taken to ensure that the resulting solution was free of Ag^+ ions and that the chloro complex had been completely converted into the aqua species. Since it is known that perchlorate ions do not coordinate to Pt^{II} and Pd^{II} in aqueous solution,[29] the kinetics of the complex-formation reactions were studied in 0.1 M $NaClO_4$ (Merck, p.a.). The pH of the solutions was adjusted to 2.5 with $HClO_4$ and NaOH, whereas for pH 4.75 a freshly prepared acetic acid/acetate buffer solution was used.

Instrumentation: Chemical analyses were performed on a Carlo–Erba Elemental Analyser 1106. UV/Vis spectra were recorded on Shimadzu UV250 and Hewlett–Packard 8452A diode-array spectrophotometers in thermostatted 1.00 cm quartz Suprasil cells. Kinetic measurements were carried out on an Applied Photophysics SX.18MV stopped-flow instrument coupled to an on-line data acquisition system. Potentiometric measurements were performed using a Metrohm 701 titroprocessor. The electrode and titroprocessor were calibrated with standard buffer solutions prepared according to NBS specifications.[30] The temperature was controlled throughout all kinetic experiments to ± 0.1 °C. All kinetic measurements were performed under pseudo-first-order conditions, i.e., at least a 10-fold excess of the nucleophile was used.

Potentiometric Measurements: The pH meter readings were converted into hydrogen ion concentration by titrating a standard acid solution (0.01 M), the ionic strength of which was adjusted to 0.1 M with $NaNO_3$, with standard base at 25 °C. When the pH is plotted against p[H], the relationship pH – p[H] = 0.05 was observed. The $[OH^-]$ was calculated using a pK_w value of 13.997.[31]

The acid dissociation constants of the ligands were determined by titrating 0.05 mM solutions of each with a standard NaOH solution. The acid dissociation constant of the coordinated water molecule in $[Pd(AEP)(H_2O)]^{2+}$ was determined by titrating 0.10 mM solution of the complex with NaOH. The formation constants of the complexes were determined by titrating solution mixtures of $[Pd(AEP)(H_2O)]^{2+}$ (0.05 mM) and the ligand in a concentration ratio of 1:1 for all ligands, except for glutathione where the concentration ratios were 1:1 and 2:1 (Pd^{II}:glutathione). The titration solution mixtures had a volume of 40 mL. The titrations were carried out at 25 °C by circulating thermostatted water through the double-wall titration vessel, and under a slow and constant stream of N_2 over the test solutions. The ionic strength was adjusted to 0.1 M by addition of $NaClO_4$. A 0.05 M NaOH solution was used as titrant. The equilibrium constants for the species of general formula $M_lL_pH_q$, [M = Pd(AEP), L = ligand], were calculated using the computer program MINIQUAD-75.[32]The stoichiometry and stability constants of the complexes formed were determined by considering various possible composition models. The model selected is accepted on the basis of chemical logic, it gave the best statistical fit as indicated by low standard deviation and sum of square of residuals, and was chemically consistent with the titration data, without giving any systematic drifts in the magnitude of various residuals, as described elsewhere.[32] The results are summarized in Table 1. The species distribution diagrams were obtained using the program SPECIES under the experimental conditions used.

Kinetics Measurements: The substitution kinetics of coordinated water was investigated spectrophotometrically. Spectral changes resulting from mixing complex and nucleophile solutions were re-

corded over the wavelength range 200 to 600 nm to establish a suitable wavelength at which kinetic measurements could be performed (see Table S1 and Figure S3 in the Supporting Information) for the nucleophiles L-met, GSH, 5′-GMP, INO and Gly. Reactions were initiated by mixing equal volumes of the complex and ligand solutions directly in the stopped-flow instrument and were followed for at least eight half-lives. All stopped-flow kinetic experiments were performed under pseudo-first-order conditions with respect to the nucleophile concentration. All kinetic runs could be fitted to a single exponential function, except for the substitution by glutathione where a double exponential function was employed to fit the kinetic traces. The observed pseudo-first-order rate constants, k_{obsd}, were calculated as the average value from five to eight independent kinetic runs and are summarized in Tables S2–S5 (see Supporting Information). The reactions were studied at pH 2.5 (0.1 M $NaClO_4$) and 4.75 (10 mM acetic acid/acetate buffer).

Quantum Chemical Calculations: We performed B3LYP/LANL2DZp hybrid density functional calculations, i.e., with pseudo-potentials on the heavy elements and the valence basis set augmented with polarization functions.[33,34] In addition, the resulting structures were characterized as minima by computation of the vibrational frequencies. The relative energies were corrected for zero point vibrational energies (ZPE). The GAUSSIAN 03 suite of programs was used.[35]

Supporting Information (see also the footnote on the first page of this article): Wavelengths at which kinetic measurements were performed (Table S1, Figure S3); Tables with pseudo-first-order rate constants (Tables S2 to S5); Figures with distribution diagrams (Figures S1 and S2).

Acknowledgments

The authors gratefully acknowledge financial support from the Ministry of Science and Technological Development, Republic of Serbia (Project No. 142008), the Deutsche Forschungsgemeinschaft (DFG) and Deutscher Akademischer Austauschdienst (DAAD) for a fellowship to M. S.. We would like to thank Prof. Tim Clark for hosting this work in the CCC and the Regionales Rechenzentrum Erlangen (RRZE) for a generous allotment of computer time.

[1] T. Rau, R. van Eldik, *Metal Ions in Biological Systems* (Eds.: A. Sigel, H. Sigel), Marcel Dekker, New York, **1996**, p. 340.
[2] a) *Cisplatin Chemistry and Biochemistry of Leading Anticancer Drugs* (Ed.: B. Lippert), Wiley-VCH, Zürich, **1999**; b) D. Wang, S. J. Lippard, *Nat. Rev. Drug Discovery* **2005**, *4*, 307–320; c) S. van Zutphen, J. Reedijk, *Coord. Chem. Rev.* **2005**, *24*, 2845–2853; d) H. Zorbas, B. K. Keppler, *ChemBioChem* **2005**, *6*, 1157–1166.
[3] E. L. J. Breet, R. van Eldik, *Inorg. Chem.* **1987**, *26*, 2517–2524.
[4] E. L. J. Breet, R. van Eldik, *J. Chem. Soc., Chem. Commun.* **1987**, 408–409.
[5] Ž. D. Bugarčić, G. Liehr, R. van Eldik, *J. Chem. Soc., Dalton Trans.* **2002**, 951–956.
[6] Ž. D. Bugarčić, G. Liehr, R. van Eldik, *J. Chem. Soc., Dalton Trans.* **2002**, 2825–2830.
[7] D. Jaganyi, F. Tiba, O. Munro, B. Petrović, Ž. D. Bugarčić, *Dalton Trans.* **2006**, 2943–2949.
[8] Ž. D. Bugarčić, S. T. Nandibewoor, M. S. A. Hamza, F. Heinemann, R. van Eldik, *Dalton Trans.* **2006**, 2984–2990.
[9] Ž. D. Bugarčić, T. Soldatović, R. Jelić, B. Algueró, A. Grandas, *Dalton Trans.* **2004**, 3869–3877.
[10] T. Soldatović, Ž. D. Bugarčić, *J. Inorg. Biochem.* **2005**, *99*, 1472–1479.
[11] N. Summa, T. Soldatović, L. Dahlenburg, Ž. D. Bugarčić, R. van Eldik, *J. Biol. Inorg. Chem.* **2007**, *12*, 461–475.
[12] Z. Guo, P. J. Sadler, E. Zang, *Chem. Commun.* **1997**, *1*, 27–28.
[13] D. Kiser, F. P. Intini, Y. Xu, G. Natile, L. G. Marzilli, *Inorg. Chem.* **1994**, *33*, 4149–4158.
[14] S. O. Ano, F. P. Intini, G. Natile, L. G. Marzilli, *J. Am. Chem. Soc.* **1997**, *119*, 8570–8571.
[15] U. Frey, J. D. Ranford, P. J. Sadler, *Inorg. Chem.* **1993**, *32*, 1333–1340.
[16] Ž. D. Bugarčić, M. M. Shoukry, R. van Eldik, *J. Chem. Soc., Dalton Trans.* **2002**, 3945–3951.
[17] Ž. D. Bugarčić, B. Petrović, E. Zangrando, *Inorg. Chim. Acta* **2004**, *357*, 2650–2656.
[18] D. D. Perrin, *Stability Constant of Metal-Ion Complexes: Part B*, Organic Ligands, Pergamon Press, Oxford, **1979**.
[19] E. L. J. Breet, R. van Eldik, H. Kelm, *Polyhedron* **1983**, *2*, 1181–1187.
[20] M. Boiocchi, M. Bonizzoni, L. Fabbrizzi, F. Foti, M. Licchelli, A. Taglietti, M. Zema, *Dalton Trans.* **2004**, 653–665.
[21] H. Sigel, S. S. Massoud, N. A. Corfu, *J. Am. Chem. Soc.* **1994**, *116*, 2958–2971.
[22] M. L. Tobe, J. Burgess, *Inorganic Reaction Mechanisms*, Addison Wesley Longman Inc., Essex, **1999**, p. 74.
[23] R. M. Smith, A. E. Martel, *Critical Stability Constants*, vol. 6, 2nd Suppl., Plenum Press, New York, NY, **1989**, p. 20.
[24] J. Arpalahti, P. Lehikoinen, *Inorg. Chem.* **1990**, *29*, 2564–2567.
[25] J. Arpalahti, B. Lippert, *Inorg. Chem.* **1990**, *29*, 104–110.
[26] Ž. D. Bugarčić, F. W. Heinemann, R. van Eldik, *Dalton Trans.* **2004**, 279–286.
[27] R. B. Martin, *Acc. Chem. Res.* **1985**, *18*, 32–38.
[28] R. Jacobs, F. Prinsloo, E. Breet, *J. Chem. Soc., Chem. Commun.* **1992**, 212–214.
[29] T. G. Appleton, J. R. Hall, S. F. Ralph, C. S. M. Thompson, *Inorg. Chem.* **1984**, *23*, 3521–3525.
[30] R. G. Bates, *Determination of pH – Theory and Practice*, 2nd ed., Wiley Interscience, New York, **1975**.
[31] *Chemistry Data Book* (Eds.: J. G. Stark, H. G. Wallace), Murray, London, **1975**, p. 75.
[32] P. Gans, A. Sabatini, A. Vacca, *Inorg. Chim. Acta* **1976**, *18*, 237–239.
[33] a) A. D. Becke, *J. Phys. Chem.* **1993**, *97*, 5648–5652; b) C. Lee, W. Yang, R. G. Parr, *Phys. Rev. B* **1988**, *37*, 785–789; c) P. J. Stephens, F. J. Devlin, C. F. Chabalowski, M. J. Frisch, *J. Phys. Chem.* **1994**, *98*, 11623–11627; d) T. H. Dunning Jr., P. J. Hay, In: *Modern theoretical chemistry: methods of electronic structure theory* (Ed.: H. F. Schaefer III), Plenum, New York, **1977**, vol. 3, chap. 1; e) P. J. Hay, W. R. Wadt, *J. Chem. Phys.* **1985**, *82*, 270; f) P. J. Hay, W. R. Wadt, *J. Chem. Phys.* **1985**, *82*, 284; g) P. J. Hay, W. R. Wadt, *J. Chem. Phys.* **1985**, *82*, 299; h) *Gaussian Basis Sets for Molecular Calculations* (Ed.: S. Huzinaga), Elsevier, Amsterdam, **1984**.
[34] The performance of the computational level employed in this study is well documented, see for example: a) M. Galle, R. Puchta, N. J. R. van Eikema Hommes, R. van Eldik, *Z. Phys. Chem.* **2006**, *220*, 511–523; b) R. Puchta, R. Meier, N. J. R. van Eikema Hommes, R. van Eldik, *Eur. J. Inorg. Chem.* **2006**, 4063–4067; c) A. Scheurer, H. Maid, F. Hampel, R. W. Saalfrank, L. Toupet, P. Mosset, R. Puchta, N. J. R. van Eikema Hommes, *Eur. J. Org. Chem.* **2005**, 2566–2574; d) P. Illner, A. Zahl, R. Puchta, N. J. R. van Eikema Hommes, P. Wasserscheid, R. van Eldik, *J. Organomet. Chem.* **2005**, *690*, 3567–3570; e) Ch. F. Weber, R. Puchta, N. J. R. van Eikema Hommes, P. Wasserscheid, R. van Eldik, *Angew. Chem.* **2005**, *117*, 6187–6192; f) Ch. F. Weber, R. Puchta, N. J. R. van Eikema Hommes, P. Wasserscheid, R. van Eldik, *Angew. Chem. Int. Ed.* **2005**, *44*, 6033–6038.
[35] M. J. Frisch, G. W. Trucks, H. B. Schlegel, G. E. Scuseria, M. A. Robb, J. R. Cheeseman, J. A. Montgomery Jr., T. Vreven, K. N. Kudin, J. C. Burant, J. M. Millam, S. S. Iyengar, J. Tomasi, V. Barone, B. Mennucci, M. Cossi, G. Scalmani, N. Rega, G. A. Petersson, H. Nakatsuji, M. Hada, M. Ehara, K. Toyota, R. Fukuda, J. Hasegawa, M. Ishida, T. Nakajima, Y.

Honda, O. Kitao, H. Nakai, M. Klene, X. Li, J. E. Knox, H. P. Hratchian, J. B. Cross, C. Adamo, J. Jaramillo, R. Gomperts, R. E. Stratmann, O. Yazyev, A. J. Austin, R. Cammi, C. Pomelli, J. W. Ochterski, P. Y. Ayala, K. Morokuma, G. A.Voth, P. Salvador, J. J. Dannenberg, V. G. Zakrzewski, S. D. Dapprich, M. C. Daniels, O. Strain, D. K. Farkas, A. D. Malick, K. Rabuck, J. B. Raghavachari, A. Foresman, J. V. Ortiz, Q. Cui, A. G. Baboul, S. Clifford, J. Cioslowski, B. B. Stefanov, G. Liu, P.Liashenko, I. Piskorz, R. L. Komaromi, D. J. Martin, T. Fox, M. A. Keith, C. Y. Al-Laham, A. Peng, A. Nanayakkara, M. Challacombe, P. M. W. Gill, B. Johnson, W. Chen, M. W. Wong, C. Gonzalez, J. A Pople: *Gaussian 03*, Revision C.02. Gaussian, Inc., CT Wallingford, **2004**.

Received: December 19, 2008
Published Online: April 8, 2009

